# Measurement of LIL Conversion Efficiency

B. Canard, R. Bossart, K. Hübner, J.H.B. Madsen, D. Pearce

## Summary

The first measurement gives the unresolved efficiency $\eta$ I(HIP.22)/ I(WL.22) up up to $Q^-$ = 58 nC. It is constant ($\eta$ = 4.4 x $10^{-3}$) up to $Q^-$ = 35nC, then evidence for decrease.

The second measurement done at $Q^- \simeq$ 27 nC gives $\eta$ = 4.7 x $10^{-3}$.

The third more detailed measurement (analogue and digital HIP.22/ VL.15) gives again $\eta$ = 4.4 x $10^{-3}$ and $\eta$ = 3.3 x $10^{-3}$ in $\Delta p/p = \pm$ 1%; the efficiency decreased from $Q^-$ = 32 nC onwards but less than expected. Three klystron power levels were used $P_{13}$ = 23, 18 (standard value), and 14 MW. Measured LIL-V non loaded energy change agrees with theory. The measured $\eta$ change with $P_{13}$ is small and rather inconsistent apparently due to measurement errors, making comparison with the expected variation, which is small, not very meaningful.

The measurements confirm that LIL consistently operates at nominal performance. It can also provide 50% more positrons than nominal. LIL W operated at 500 MeV.

## 1. First Measurement (15. 11. 1988)

### 1.1 Question

Is the positron pulse charge always proportional to the electron pulse charge or is there a saturation at higher intensities owing to the energy spread of the electrons that is created by the beam loading and that destroys the focusing of the $e^-$ beam at the end of the pulse?

1.2 Method: Measure peak currents $I^-_{22}$ (Σ VL.UMA22), $I^+_{22}$ (Σ HIP.UMA22).

1.3 Conditions: $e^-$ beam with standard focus on target.

Klystron 13: $U_{KL}$ = 257 kV (TV) U(PKI13) = 0.72 V P = 17.4 MW

Klystron 03: $U_{KL}$ = 188 kV (TV) U(PKI03) = 2.1 V

E (LIL V) = 210 MeV from position of maximum at VL.MSH15 at $Q^-$ = 33nC

E (LIL W) = 500 MeV

## 1.4 Results

Main result: see Fig. 1.1. Measurement up to $Q^- = 58$ nC (30 nC nominal). The present settings of the vacuum interlock at SNP25 do not allow higher $Q^-$. In both cases, weak evidence for saturation from $I^- = 1.5$ A $\equiv Q^- = 35$ nC onwards. Conversion efficiency drops to 65% from $4.4 \times 10^{-3}$ (fit through lowest five · points) to $2.8 \times 10^{-3}$ (fit through last three · points). Further:

- Switching off SNP25 (2.9 kA) makes $I^+$ drop to half (see point Δ).
- Fig. 1.2 data give a pulse length $\Delta t = 23$ ns derived from the fit through the first 4 points and using

  $$\Delta t = \partial Q / \partial I$$

  This checks with the FWHH taken from Fig. 1.3

  $$\Delta t = 22 \text{ ns}.$$

  By the way. $\Delta t_{rise} = 8$ ns, $\Delta t_{fall} = 4$ ns for 10% to 90% in Fig. 1.3. The meter in RA017 was at $\Delta t = 25$ ns. The $e^-$ intensity was adjusted by varying the pulse height of the cathode pulse ("HT").
- The number of electrons in VL.UMA22 indicated by the control computer saturates at

  $$N^- = 21 \times 10^{10}$$

  though we were in $e^+$ production mode. This is too close to the nominal $N^- = 19 \times 10^{10}$. Something wrong, at least on this evening.
- The slits before HIP.UMA22 were retracted. Hence, all positron intensities are unresolved. Comparison of Fig. 1.3, Fig. 1.4 and Fig. 1.5 shows that later part of unresolved $e^+$ pulse (Fig. 1.5) was not corrupted by the expected bad focusing of the $e^-$ in the later part of the pulse.

## 2. Second Measurement (11. 12. 1988)

B. Canard measured with the standard $P_{13} = 17.4$ MW, after optimisation, the peak analogue signals Σ (HIP.22)/ Σ(WL.22) with the momentum-defining slits open

$$\eta = I^+_{22} = 6.7 \text{ mA} / 1.4 \text{ A} = 4.7 \times 10^{-3}$$

The $e^-$ current in WL.25 was only 1.2 A showing the wellknown but not explained offset between WL.22 and WL.25. Since WL.22 always agrees with VL.15, we ignore WL.25.

## 3. Third Measurement (12. 12. 1988)

3.1 Purpose Find influence of klystron 13 power on $e^+$ production.

3.2 Primary beam

Table 1 gives the data pertaining to the klystrons. The measurements were done with three power levels of klystron 13: $P_{13}$ = 23.3; 17.7; 14.0 MW. Parameters shown in the first 3 columns. During the measurement the power was adjusted by choosing the appropriate input power. The klystron voltage was kept constant. We preferred this mode of power adjustment because it allowed for nearly the same rf phases within 3° independent of the power level (cf. table 1). We had noticed that adjustment of $P_{13}$ via the voltage required readjustment of $\varphi_{13}$. The last column in table 1 gives the initial standards parameter. It includes a power measurement after the detuned LIPS cavities, showing that PLI is only 7% lower than PKI, which is a useful cross-check.

Table 1 also gives the maximum energy, i.e. non-load energy of LIL-V derived from the spectra measured at low intensity (2.5 nC). Fig. 3.1 shows the plot $E_{max} = f(\sqrt{P_{13}})$. The l.s.q. fit yields

$$E_{max}\ (\text{MeV}) = 46.3\ \sqrt{P_{13}}\ (\text{MW}) + 33.9\ \text{MeV} \qquad (1)$$

The expected relation is for LIPS timing at optimum and $P_{03}$ = 10.4 MW

$$E_{max}\ (\text{MeV}) = 44.9\ \sqrt{P_{13}}\ (\text{MW}) + 25.6\ \text{MeV} \qquad (1)$$

where we took into account the properly weighted attenuation between klystrons and accelerating structures. The first term giving the energy gain in ACS 11, 12, 13, 14 is within 3% the same in (1) and (2). The second term corresponding to the gain in the buncher is different in (1) and (2) but the error is acceptable as the fit is made over a relatively narrow range in power. If the slope were lower by 4% in (1), the second term would agree.

Beam position x,y, and FWHH size $\Delta x$, $\Delta y$ before the targets are given in table 2. They are derived from the WBS 25 scans given in Fig. 3.2 a, b, c. It is not understood why $\Delta x$ is so large at 17.7 MW and $\Delta y$ at 23.3 MW. Also the traditional offset in y remains unexplained (target or WBS 25 position wrong).

The quadrupolet settings are given at the end of table 2, and in table 3 is shown by how much the settings had to be changed to get maximum positron production (10% changes only). The beam parameters at this optimum are also given in table 2 for 17.7 MW. It can be seen that the beam size was reduced to 60% leading to a production increase of 10%, which shows that the positron yield is not very sensitive to the spot size once it is $< 2$ mm.

Unfortunately, all quadrupole settings for 17.7 MW and 14.0 MW are doubtful as logbook and notes on graphs disagree. Also the logic behind the choice of settings in table 2 could not be reconstructed. Originally, we intended to have one standard setting for all power levels. As will be shown later, the influence of $P_{13}$ is small and the fact that we did not have the same settings will obscure the results.

3.3 Positron intensity versus electron intensity (measurements)

Intensity measurements: electrons at $\Sigma$ (VL. UMA15)

positrons at $\Sigma$ (HIP.UMA15)

Peak analogue values and digital values recorded.
VL.UMA22 and 25 not operational: victims of last LIL timing problems.
Positrons with HIP slits open and closed to aperture of 14 mm, which corresponds to $\pm$ 1%.

a) Plots of $\Sigma^+_{22} = f(\Sigma^-_{15})$ analogue peak value in Fig. 3.3 a, b, c. Dashed lines are least-square fits. Note good proportionality. Slope yields conversion efficiency $\eta$ given in table 4 first two columns. Fig. 3.4 shows $\eta$ versus $E \simeq \sqrt{P_{13}}$ as we expect that $\eta$ is a linear function of $\sqrt{P_{13}}$ to first approximation.

b) Plot of $\Sigma^+_{22} = f(\Sigma^-_{15})$ digital values in Fig. 3.5, a, b, c. Dashed lines are fits over whole range in Fig. 3.5 a; fits are only through 4 lowest points in Fig. 3.5 b and 3.5 c. Note saturation from about $N^- = 2 \times 10^{11}$ onwards in the last two cases. Slope of fits yields $\eta$ given in table 4 last two columns; in parenthesis $\eta$ corresponding to

highest intensity. Plot of $\eta$ in Fig. 3.6. Table 5 gives $\eta$ relative to the value at 17.7 MW our standard. Analogue and digital value show different absolute values and behaviour for same slit condition, but also comparing the case slits out and slits in for the same measurement method does not give a consistent picture. The resolved $\eta$ is 75% of the unresolved $\eta$ in agreement with other measurements[1]. In all three measurements, the rf phases were kept constant but, unfortunately, the quadrupole settings are slightly different (cf. table 2).

## 3.4 Positron energy spectrum

Fig. 3.7 shows the spectrum with $P_{13}$ = 23.3 MW as example. The spectrum is independent of $P_{13}$ level as expected. It has a FWHH of 5.8 MeV ≡ 1.1%. Note that the bucket height in EPA with the usual 40 kV is ± 1.5%.

## 3.5 Observation of pulse shapes of positrons

At 23.3 MW, the $e^+$ pulse shape HIP.UMA22 was independent of current and whether slits were in or out. At 14 MW, the pulse got distorted above 1.7 x $10^{11}$ $e^-$ independent of slit position as shown in Fig. 3.8, 3.9, 3.10. The pulse could be made square by adjusting the phase 03 but at the same time the pulse height was decreased by about 20%. Whether this difference in behaviour is really correlated to $P_{13}$ is very doubtful.

Plot of $N_{15}$ versus $\hat{I}_{15}$ (not shown) is linear, no saturation. From the slope we deduce a pulse width according to

$$\Delta t = \partial Q/\partial \hat{I} = 19 \text{ ns}.$$

## 3.6 Comparison with nominal and design performance

Primary beam $N^-$ = 1.88 x $10^{11}$ $Q^-$ = 30 nC nominal = design

Positron beam $N^+$ = 6 x $10^8$ $Q^+$ = 96 pC nominal in ± 1%

Positron beam $N^+$ = 9 x $10^8$ $Q^+$ = 144 pC design in ± 1%

We use the definitions of the LEP Design Report Vol. 1. Nominal: performance required for nominal operation of LEP injection chain; design performance: design aim for linac.

From the plots Fig. 3.5 a, b, c it is clear that LIL has the nominal performance in terms of charge. The pulse width is 19 ns instead of 12 ns but EPA does not mind the larger width according to our experience (cf. also forthcoming report by Hübner and Potier). It could be that 12 ns works as well, simply not tried.

The design intensity was virtually reached with 23.3 MW (cf. Fig. 3.5 a). However, in order to obtain it, we needed 43 nC in the primary pulse, i.e. 44% more electrons. Thus, design conversion efficiency not reached in this experiment.

## 3.7 Expected performance

We expect the conversion efficiency to scale as

$$\eta = q/Q_{15} \backsim (E - E_1) \qquad (3)$$

from the production cross-section where $E_1$ = 25 MeV[2]. Define

q - positron charge

E - average electron energy

$Q_i$ - electron charge at $VL.UMA_i$

$E_{max}$ - non-load electron energy

Q - average charge in ACS 11 to 14

a - beam loading factor $\partial E/\partial Q$ per section, $a_b$ for buncher

b - index for buncher V

We neglect in (3) the defocusing of the electron beam on the target by energy changes and by beam loading. Hence, in this approximation

$$\eta \backsim \left[ E_{max} - E_1 - Q_{15} \left( a \frac{Q}{Q_{15}} + a_b \frac{Q_b}{Q_{15}} \right) \right] \qquad (4)$$

Using the transmission measurement at a mean intensity $Q_{15}$ = 28 nC given in table 8 yields

$$Q/Q_{15} = \sum_{I=11}^{15} (1/5)\, Q_i/Q_{15} = 1.1 \qquad Q_b/Q_{15} \simeq Q_{11}/Q_{15} = 1.3$$

$$\eta \backsim \left[E_{max}\ (\text{MeV}) - 25\ \text{MeV} - Q_{15}\ (\text{nC}).0.95\right] \qquad (5)$$

This information is now used to discuss the effect of the klystron power $P_{13}$ and the effect of the primary charge $Q_{15}$ on $\eta$.

a) Klystron power $P_{13}$

Table 6 gives in the third column the expected change of $\eta$ in the limit of vanishing intensity $Q_{15}$ relative to $P_{13}$ = 17.7 MW. The expected change is relatively small. Comparison with the measured values without parenthesis in table 5 shows no agreement. This may be partly due to the fact that the real effect is masked by the effect of the quad changes (cf. table 3), both effects being of the same size.

We may also consider the conversion efficiency at $Q_{15}$ = 45 nC $\equiv$ N = 2.8 x $10^{11}$. Measured relative values in parenthesis in table 5, expected relative values in fourth column of table 6. Although measured tendency except value at 14 MW with slits out correct, we are far from agreement, maybe again for the reason given above.

b) Effect of primary charge

Table 7 gives the values to be compared. We expected that theoretical values neglecting the focusing change would be larger than the experimental ones. This is not the case, but at least the tendency is correct.

3.8 Proposal

- Repeat experiment but keep quads constant;
- Repeat experiment varying $P_{13}$; optimize $\varphi_{13}$ each time; keep $Q^-$ constant. Repeat with quads optimized at each $P_{13}$ level.

References

1) J.H.B. Madsen et al., "Results in MD's in Autumn 1988 on $e^+$", PS/LP Note 89-04

2) Aggson and L. Burnod, LAL report 27 (1967)

3) A. Riche, "Measurements made on LP when running for high intensity $e^+$ beam for SPS", LP Note 88-65

Table 1, RF power generation data for klystron 13 and rf phase

| | | | | | |
|---|---|---|---|---|---|
| P (PKI 13) = $P_{13}$ | MW | 23.3 | 17.7 | 14.0 | 17.4 |
| P (PLI 13) | MW | - | - | - | 16.3 |
| $E_{max}$ | MeV | 258 | 227 | 208 | - |
| P (PPI 13) | W | 163 | ? | 64 | 145 |
| U (KLY) | kV | 276 | 276 | 276 | 257 |
| U (REF) | kV | 38 | 38 | 38 | 35 |
| Phase 03 | degr. | 140 | 138 | 138 | - |
| Phase 13 | degr. | 340 | 343 | 434 | - |
| Phase 25 | degr. | 155 | 155 | 155 | - |
| Phase 27 | degr. | 128 | 128 | 128 | - |
| Phase 31 | degr. | 72 | 70 | 70 | - |
| Phase 35 | degr. | 267 | 267 | 267 | - |

Table 2, Primary electron beam; position and size at WBS25
Values in parenthesis for optimum quad settings

| $P_{13}$ | MW | 23.3 | 17.7 | 14.0 |
|---|---|---|---|---|
| x | mm | - 0.16 | - 0.1 (+ 0.2) | + 0.2 |
| y | mm | + 1.6 | + 1.8 (+ 1.7) | + 1.6 |
| $\Delta x$ | mm | 1.0 | 2.2 (1.3) | 1.3 |
| $\Delta y$ | mm | 2.5 | 0.9 (0.6) | 0.9 |
| $N^-$ | VL.UMA15 | $1.72 \times 10^{10}$ | $1.71 \times 10^{10}$ | $1.75 \times 10^{10}$ |
| QLB 1514 | A | 54.0 | 50.7 (54)? | 50.7 ? |
| QLB 1523 | A | 50.7 | 52.0 (52)? | 54.0 ? |

Table 3, Optimisation of positron field at $N^-_{15} = 1.7 \times 10^{11}$

| $P_{13}$ MW | Positrons before | Positrons after opt. | QLB 1514 change A | QLB 1523 change A |
|---|---|---|---|---|
| 23.3 | $6.7 \times 10^8$ | $7.5 \times 10^8$ | 54.0 → 51.0 | 50.7 → 52.0 |
| 17.7 | 68 mV | 74 mV | ? 50.7 → 54.0 ? | ?52.0 → 52.0? |
| 14.0 | no change | | 50.7 ? | 54 ? |

Table 4, Measured conversion efficiency

| $P_{13}$ MW | η (slits out) x $10^3$ | η (slits ± 1%) x $10^3$ | η (slits out) x $10^3$ | η (slits ± 1%) x $10^3$ |
|---|---|---|---|---|
| 23.3 | 3.57 | 2.73 | 4.31 (4.11) | 3.13 (3.13) |
| 17.7 | 3.24 | 2.65 | 4.39 (3.53) | 3.29 (2.81) |
| 14.0 | 3.67 | 2.72 | 4.07 (3.77) | 3.21 (2.68) |
| | from analogue measurement | | from digital readout | |

Table 5, Relative measured conversion efficiency in %

| $P_{13}$ | analogue measurement | | digital readout | |
|---|---|---|---|---|
| MW | η (slits out) | η (slits ± 1%) | η (slits out) | η (slits ± 1%) |
| 23.3 | 110 | 103 | 98 (116) | 95 (111) |
| 17.7 | 100 | 100 | 100 (100) | 100 (100) |
| 14.0 | 113 | 103 | 93 (107) | 98 (95) |
| | from analogue measurement | | from digital readout | |

Table 6, Expected relative conversion efficiency (effect of $P_{13}$)

| $P_{13}$ MW | $E_{max}$ MeV | η ($P_{13}$)/η (17.7 MW) for $Q^- \to 0$ | η ($P_{13}$)/η (17.7 MW) for $Q^-$ = 45 nC |
|---|---|---|---|
| 23.3 | 258 | 115 % | 120% |
| 17.7 | 227 | 100 % | 100% |
| 14.0 | 208 | 91 % | 88 % |

Table 7, Ratio $\eta$ (Q = 45 nC) / $\eta$ (Q = 0)

| $P_{13}$ MW | experimental slits out | experimental slits in | theoretical |
|---|---|---|---|
| 23.3 | 0.95 | 1.0 | 0.80 |
| 17.7 | 0.80 | 0.85 | 0.77 |
| 14.0 | 0.93 | 0.84 | 0.74 |

Table 8, Example of transmission in LIL-V at about nominal charge ($P_{13}$ = 23.3 MW)

| Monitor | Particles/pulse x $10^{-13}$ | Charge/pulse nC | Relative to 15 % |
|---|---|---|---|
| ECM 01 | 4.13 | 66 | 236 |
| WCM 11 | 2.25 | 36 | 129 |
| WCM 12 | 1.85 | 30 | 107 |
| UMA 13 | 1.81 | 29 | 104 |
| WCM 14 | 1.87 | 30 | 107 |
| UMA 15 | 1.72 | 28 | 100 |
| UMA 22 | 1.82 | 29 | 104 |
| UMA 25 | 1.50 | 24 | 86 |

Distribution:

Y. Baconnier, S. Battisti, R. Bossart, B. Canard, R. Clare,

J.P. Delahaye, K. Hübner, H. Kugler, A. Krusche,

P. Lecoq, J.H.B. Madsen, D. Pearce, A. Pisent,

J.P. Potier, A. Poncet, A. Riche, L. Rinolfi, D.J. Warner

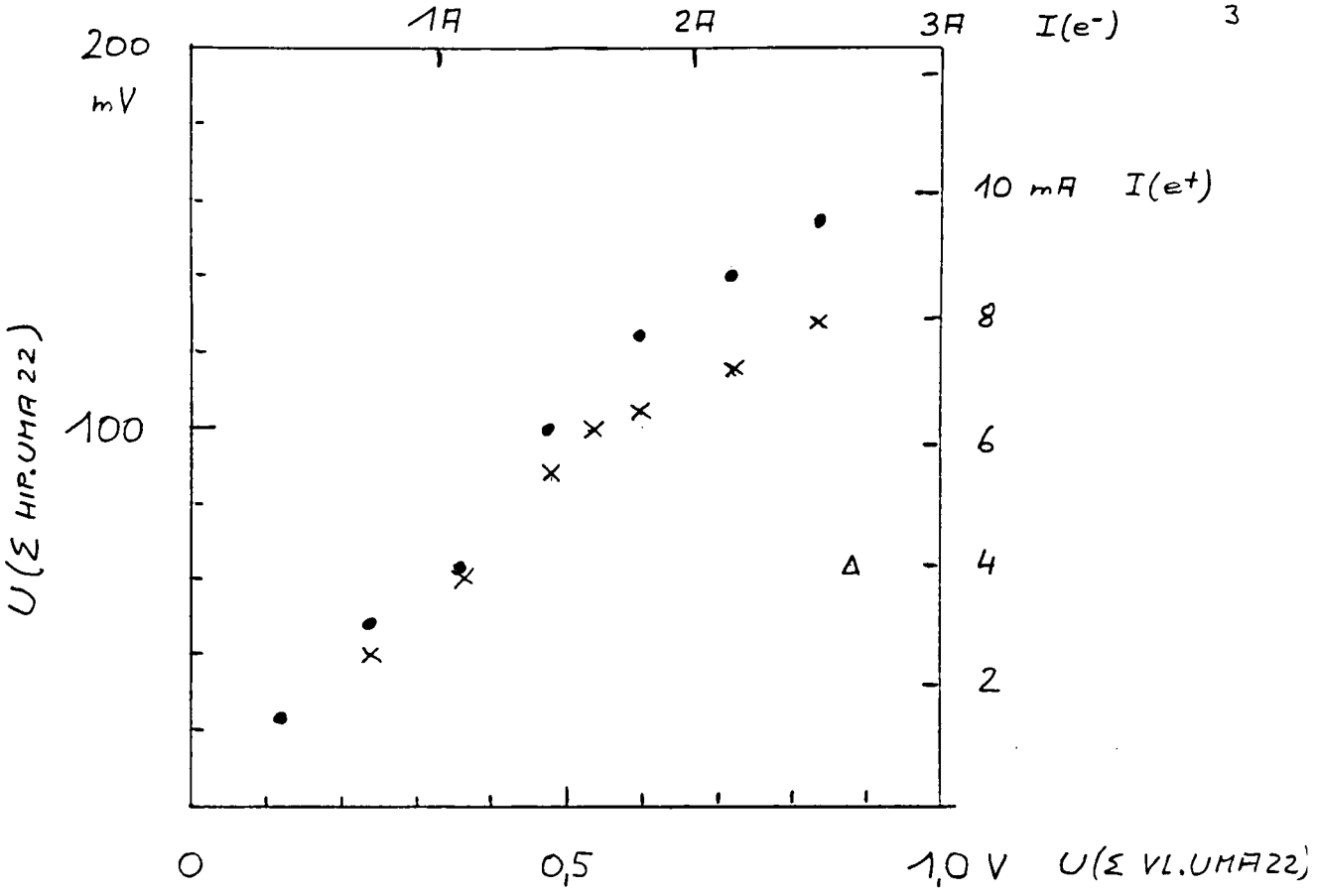


**Fig.1.1** Positron peak current versus electron peak current (analogue)
Before phase 03 adjustment Δ - SNP25 off × - SNP on (2.9 kA)
After phase 03 adjustment • - SNP on

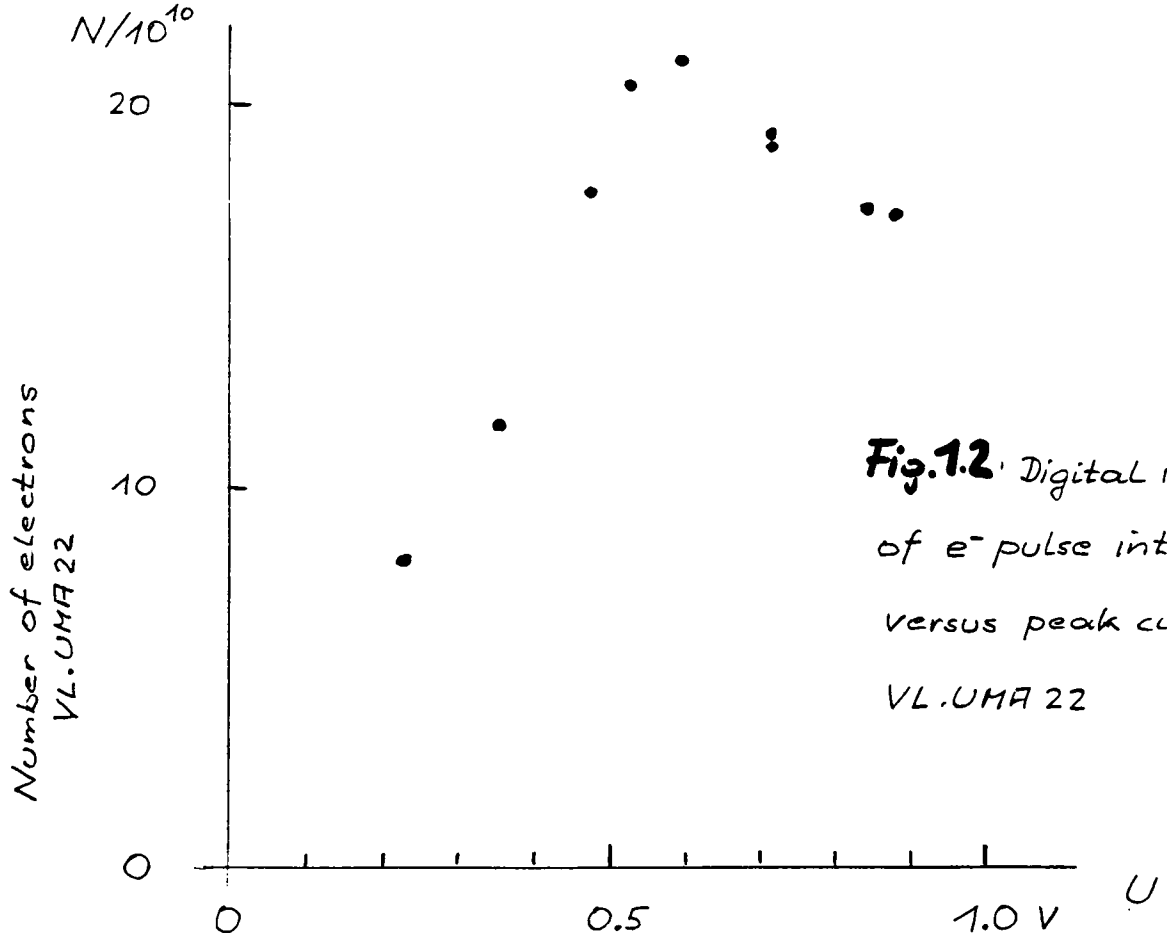


**Fig.1.2** Digital read-out of e⁻ pulse intensity versus peak current at VL.UMA 22

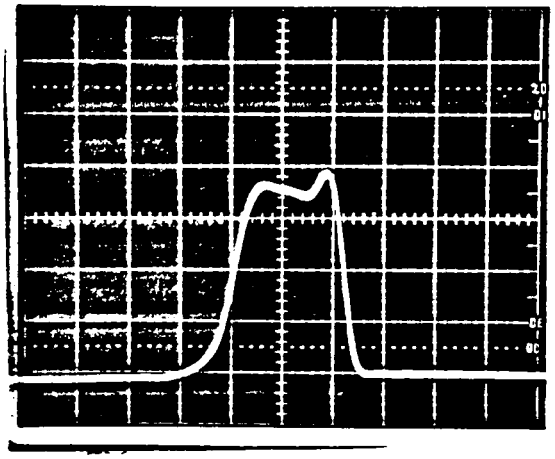

**Fig.1.3**

$\Sigma$ $e^-$ Signal VL.WCH14

50 mV/D

10 ns/D

$\hat{I} \approx 1.8A$ $Q \approx 40nC$

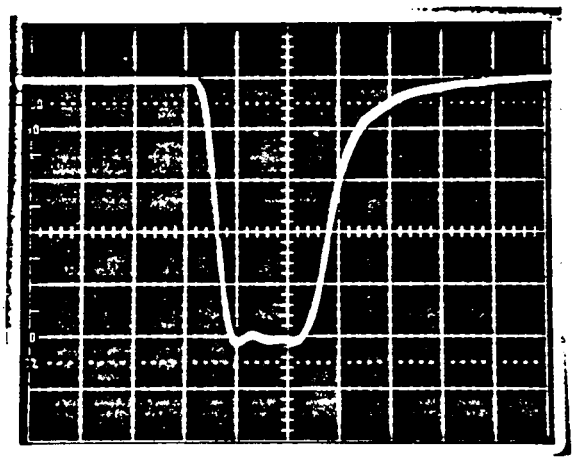

**Fig.1.4**

$\Sigma$ $e^-$ signal VL.UMA22

0.1 V/D

10 ns/D

$\hat{I} \approx 1.5A$ $Q \approx 35nC$

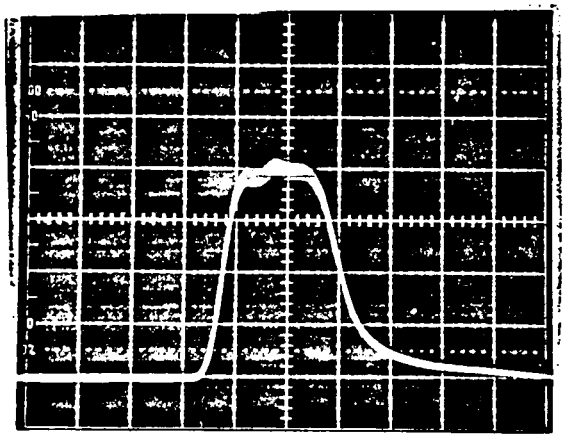

**Fig.1.5**

$\Sigma$ $e^+$ signal HIP.UMA22

20 mV/D

10 ns/D

$\hat{I} \approx 4.8mA$ $Q \approx 0.11nC$

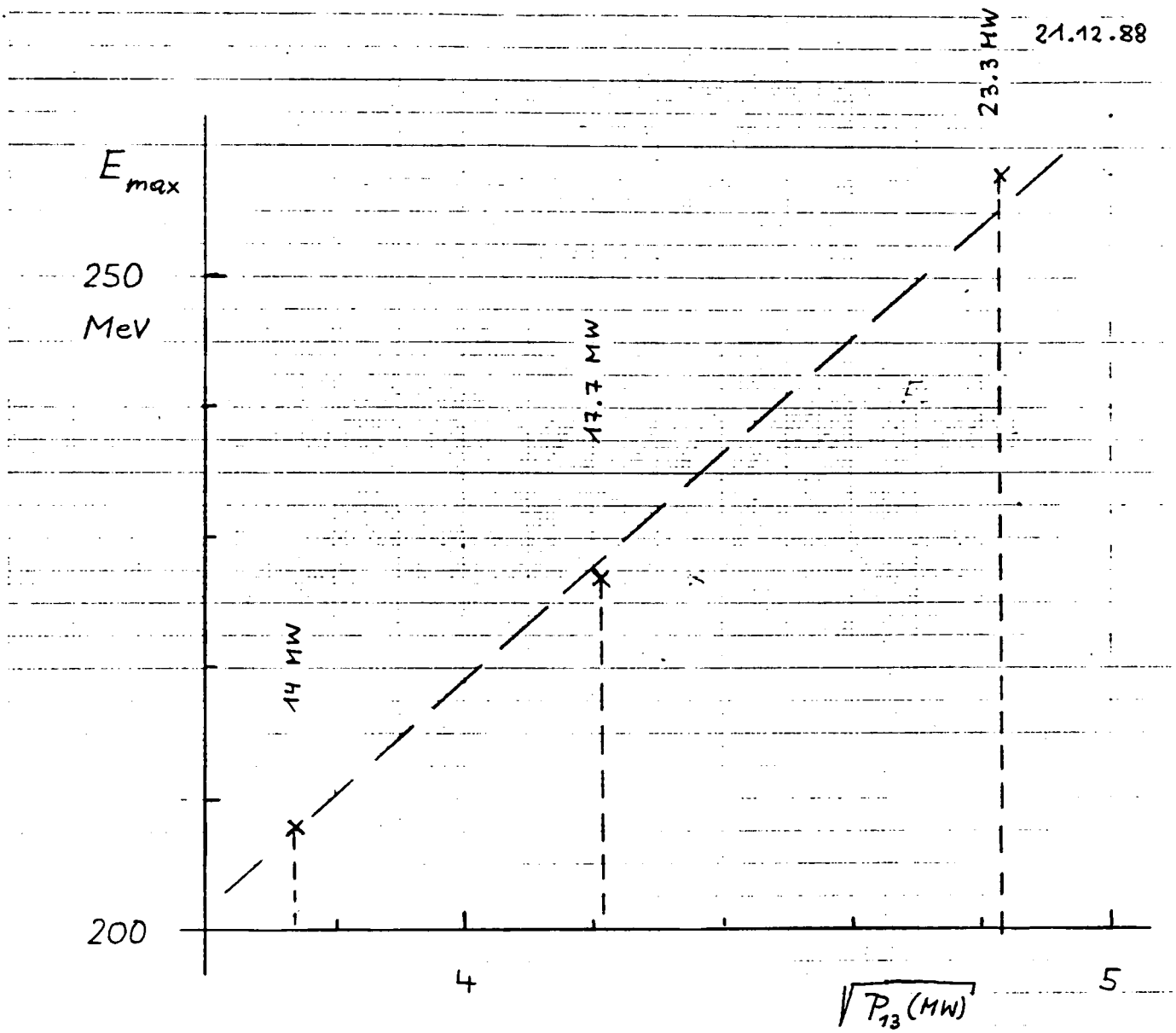


Fig. 3.1

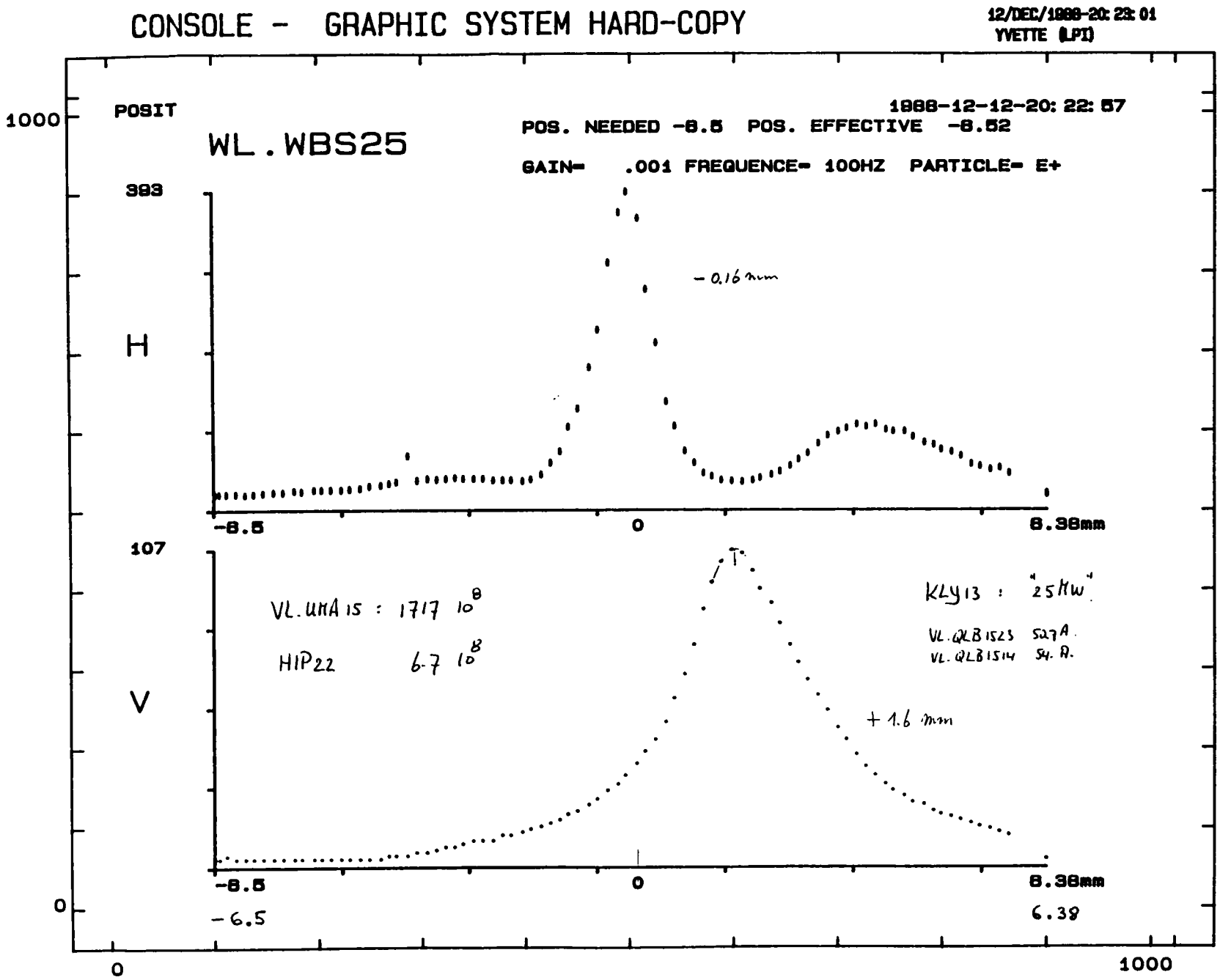


and current meas -

QLB1523 50.7 A
QLB1514 54.

Voir LIL UMA 12-17-20:20:43

$\Delta x = 1{,}0$ mm FWHH

$\Delta y = 2{,}5$ mm FWHH

$P_{13} = 23.3$ MW

Fig. 3.2a

«1514 51A

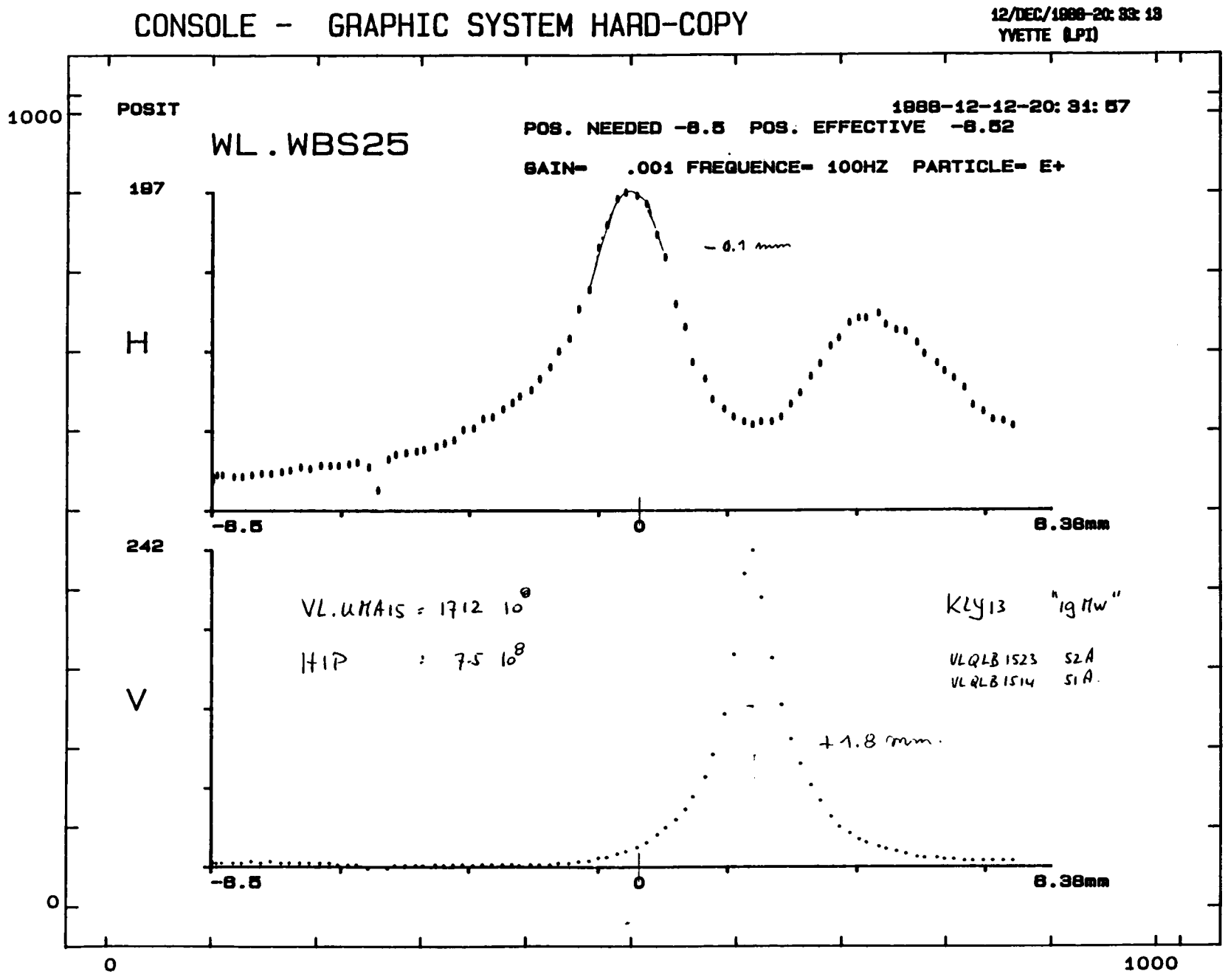


$\Delta x = 2.2$ mm
FWHH

$\Delta y = 0.94$ mm
FWHH

$P_{13} = 17.7$ MW

Fig. 3.2b

Fig. 3.2c

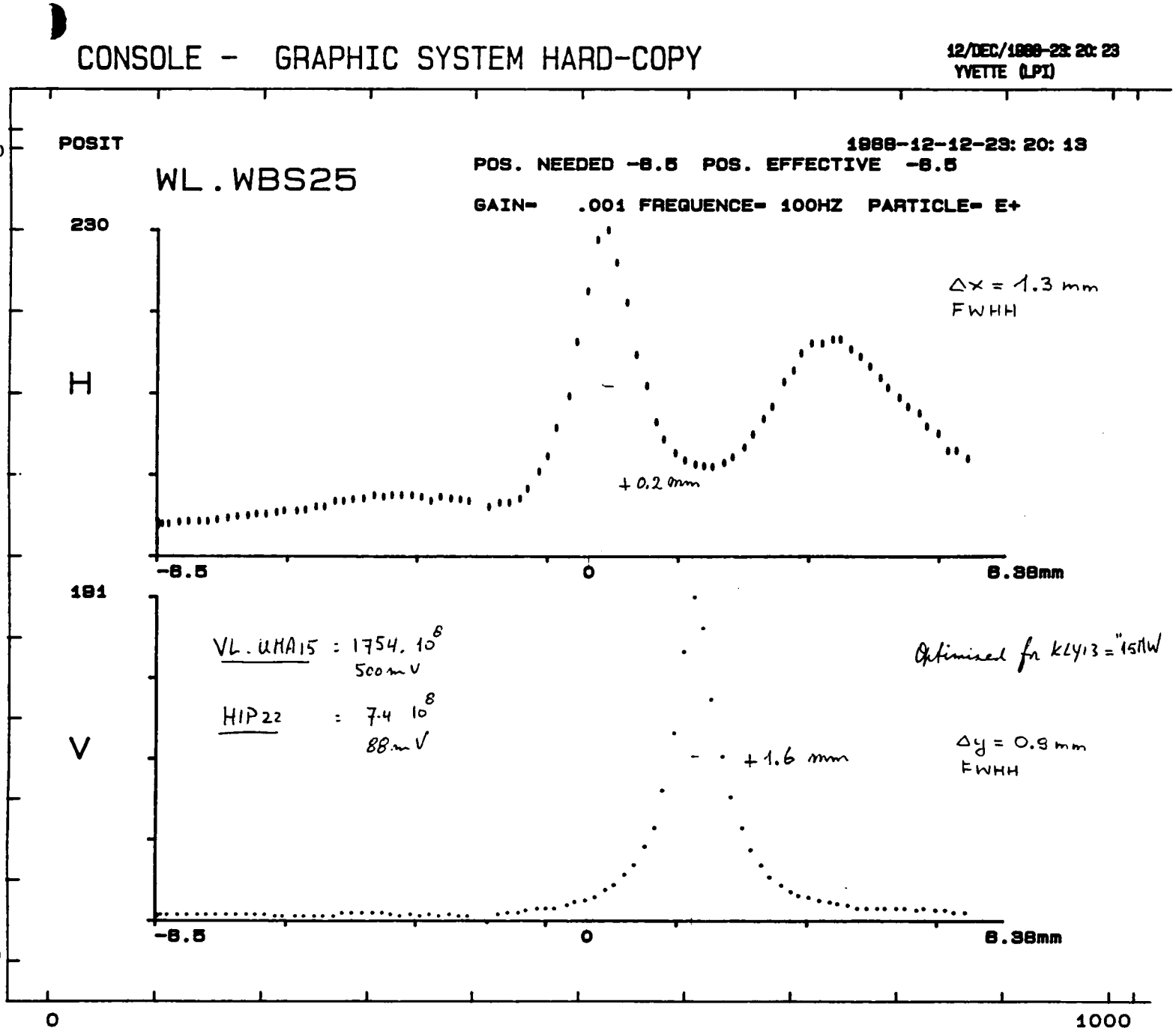


$P_{13}$ = 14.0 MW

Fig. 3.2c

12.12.88

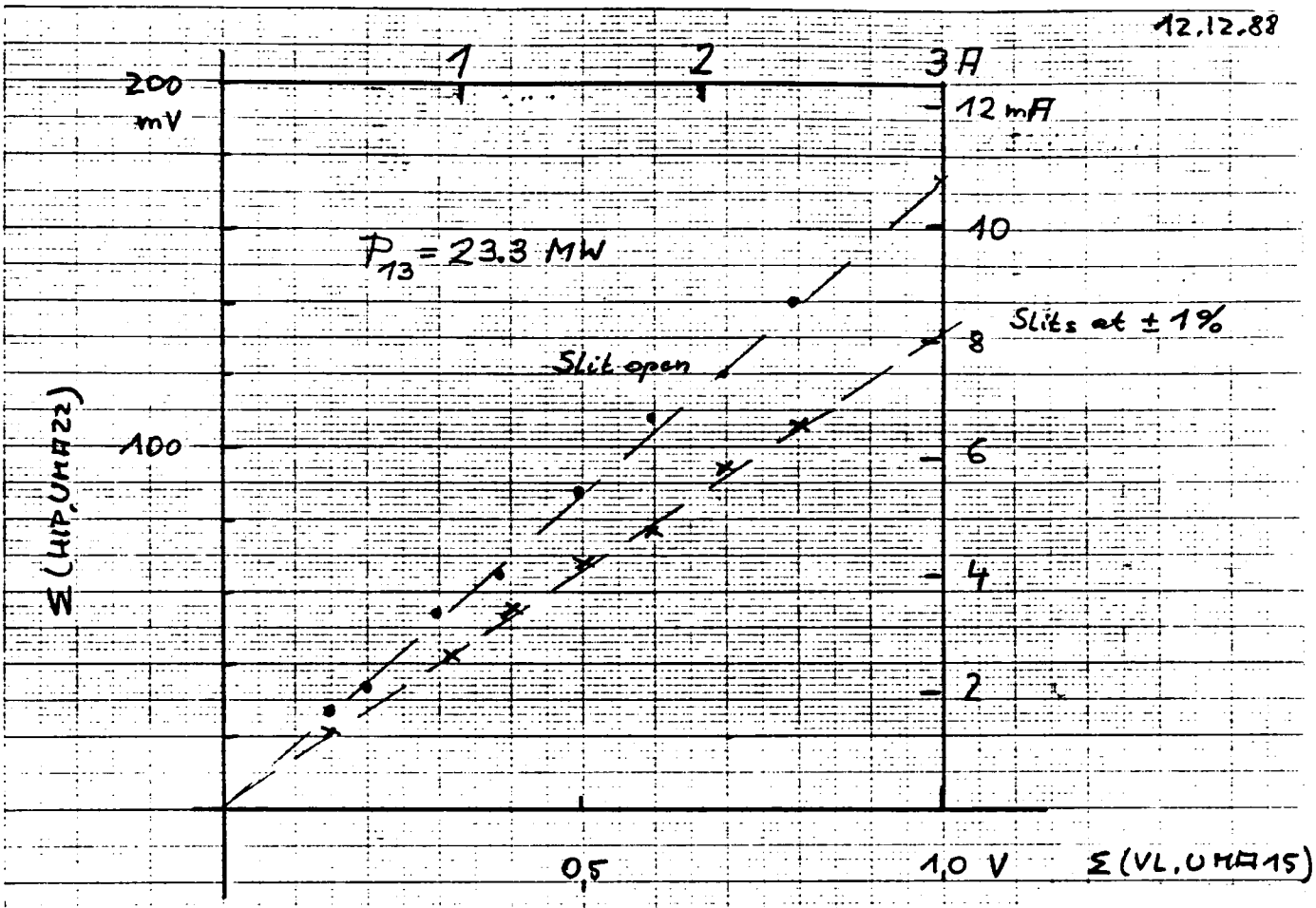


Fig. 3.3a

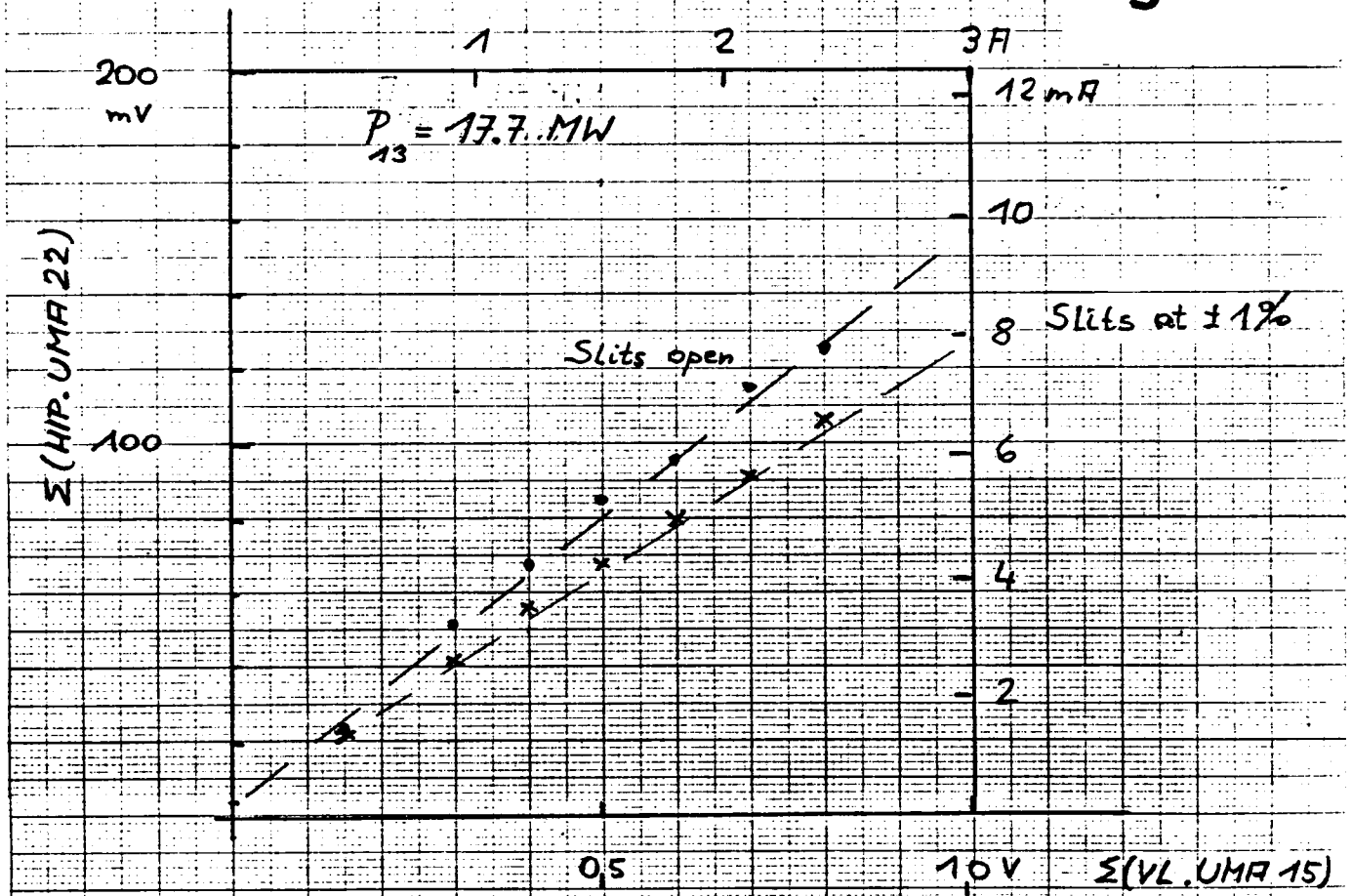


Fig. 3.3b

emil-leuch ag 3097 liebefeld bern

12.12.88

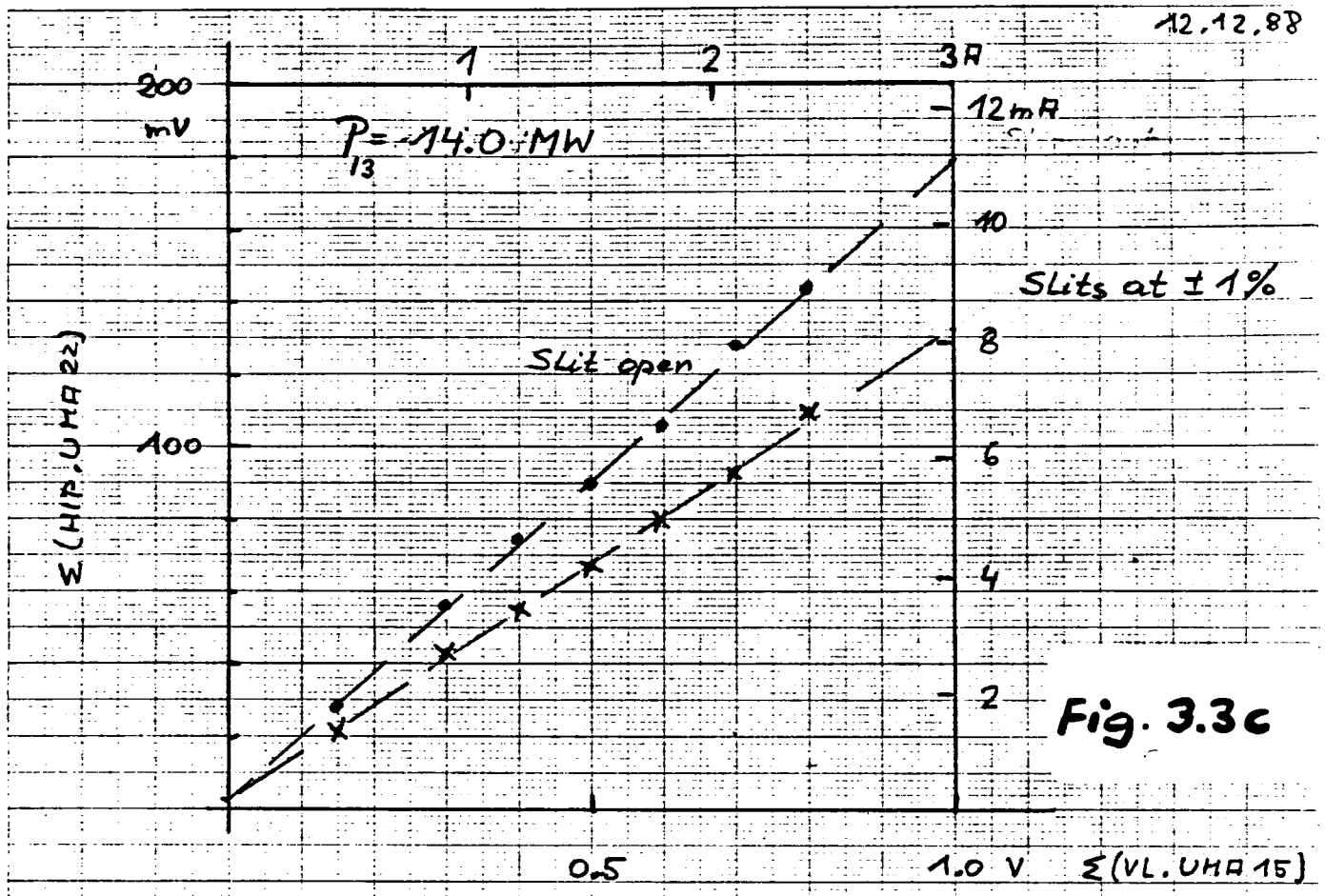


Fig. 3.3c

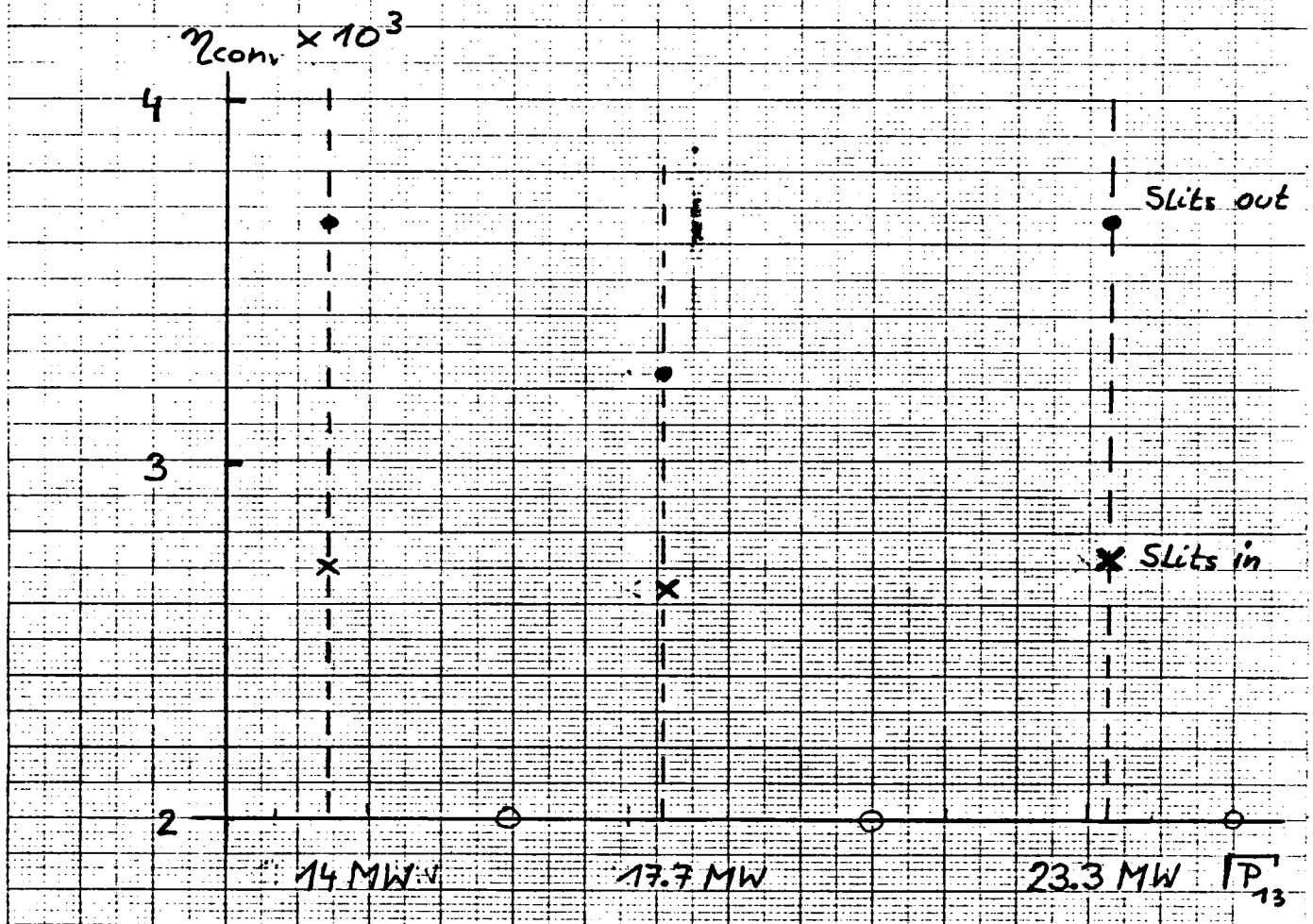


Fig. 3.4

Convesion efficiency from peak current measurements versus $\sqrt{P_{13}}$.

emi-leuch ag. 3097 liebefeld ber.

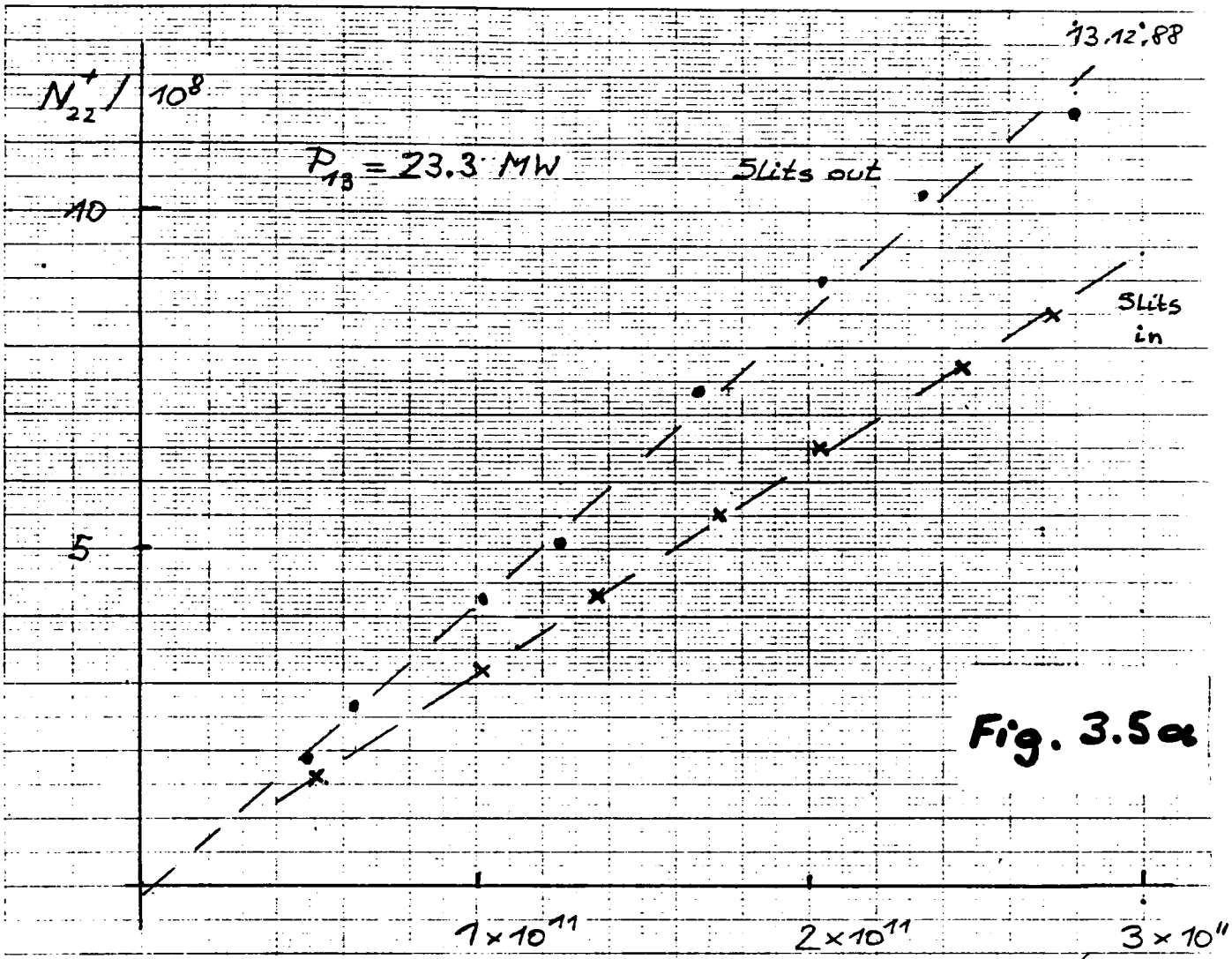


Fig. 3.5a

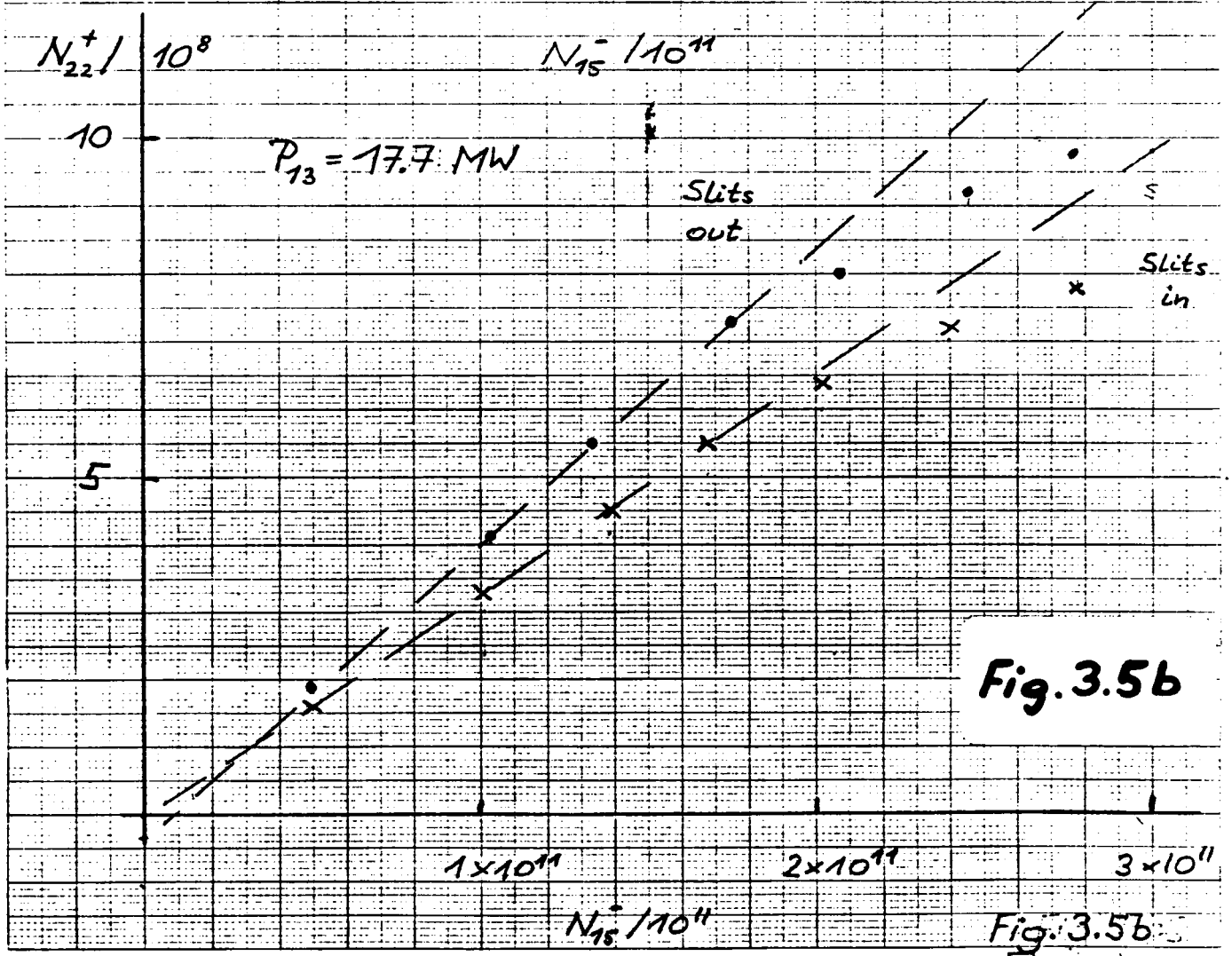


Fig. 3.5b

Fig. 3.5b

ami-touch ag 3097 liebefeld bern

13.12.88

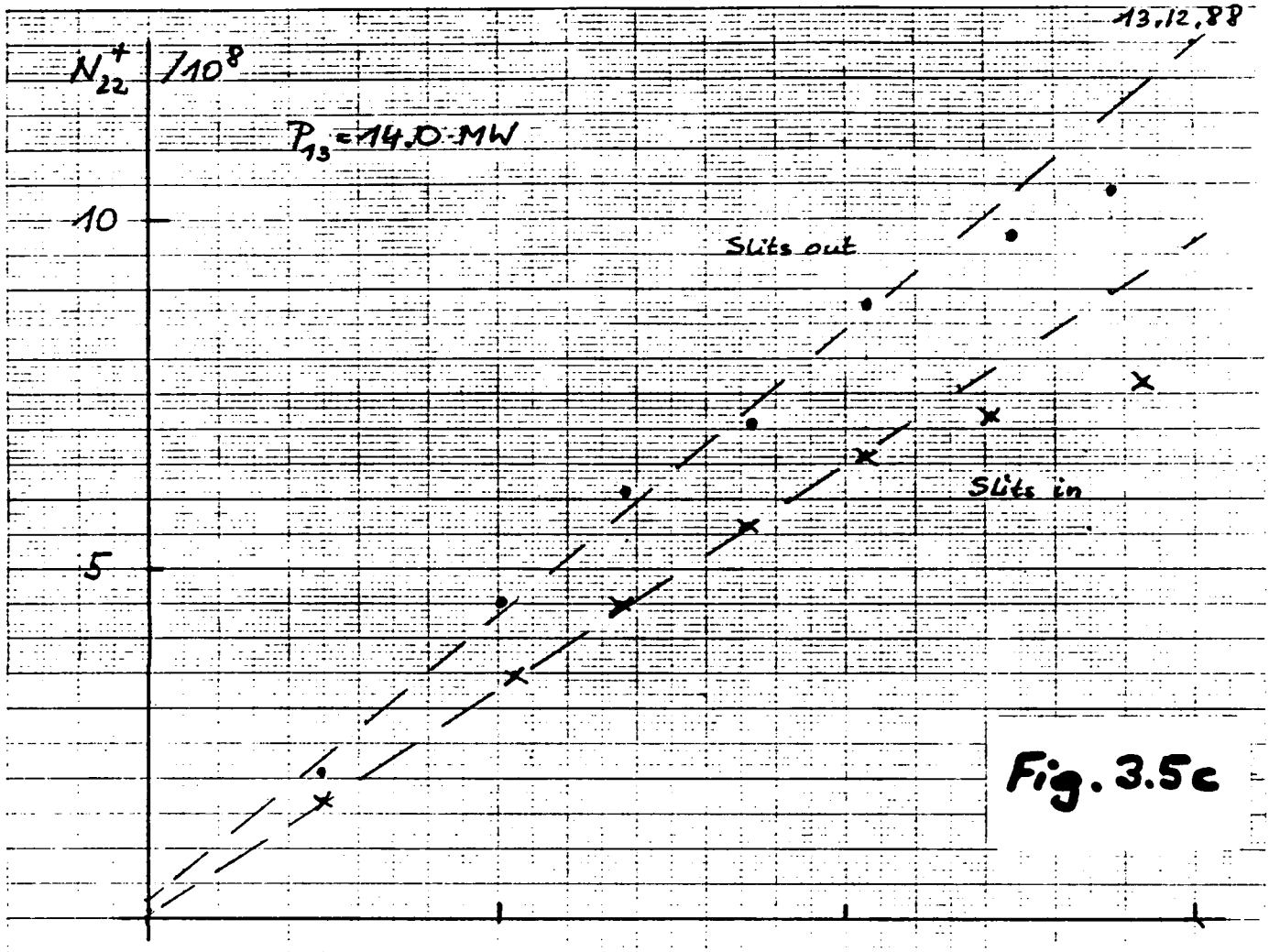


Fig. 3.5c

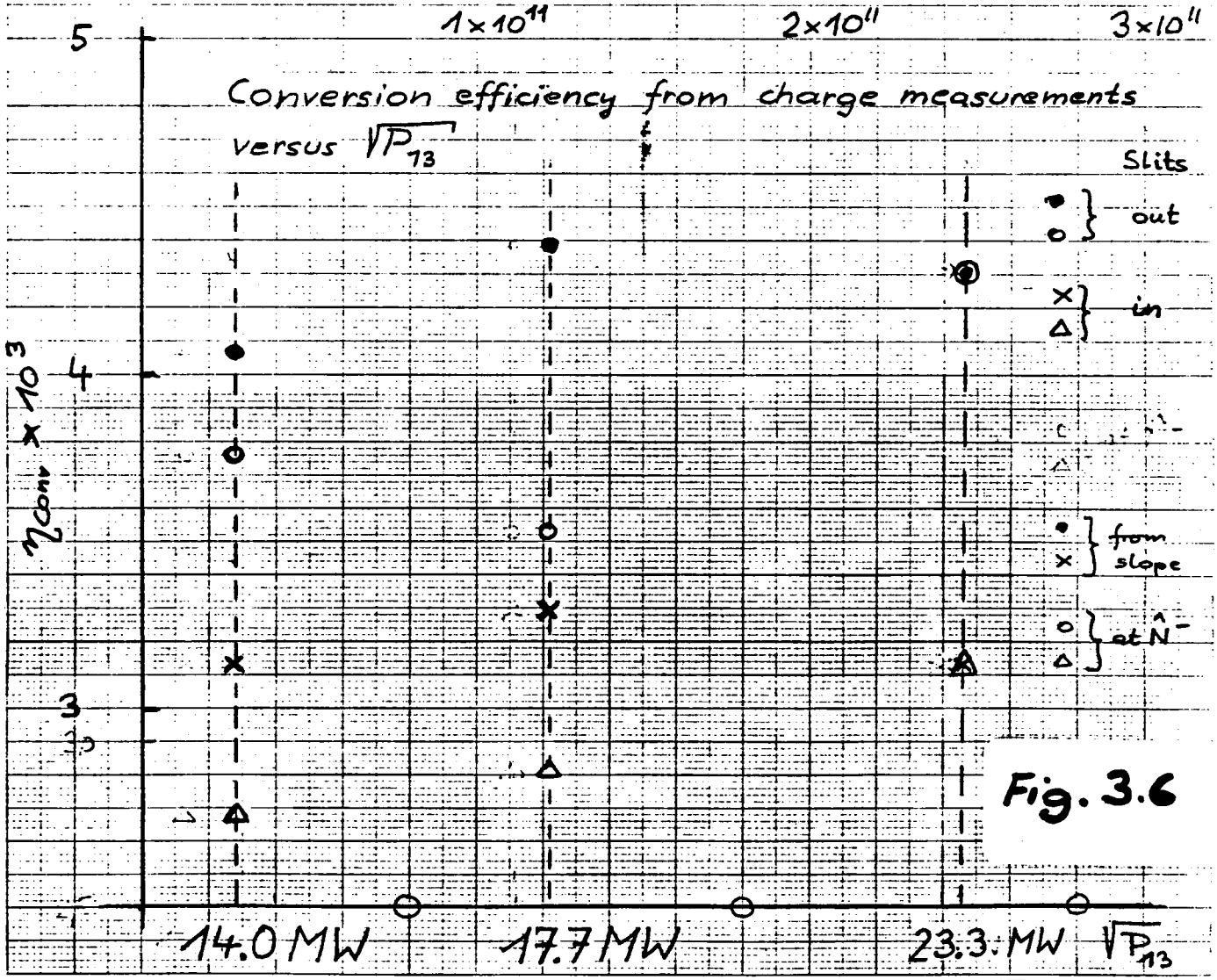


Fig. 3.6

emi-leuch ag 3097 liebefeld-bern

Fig. 3.7

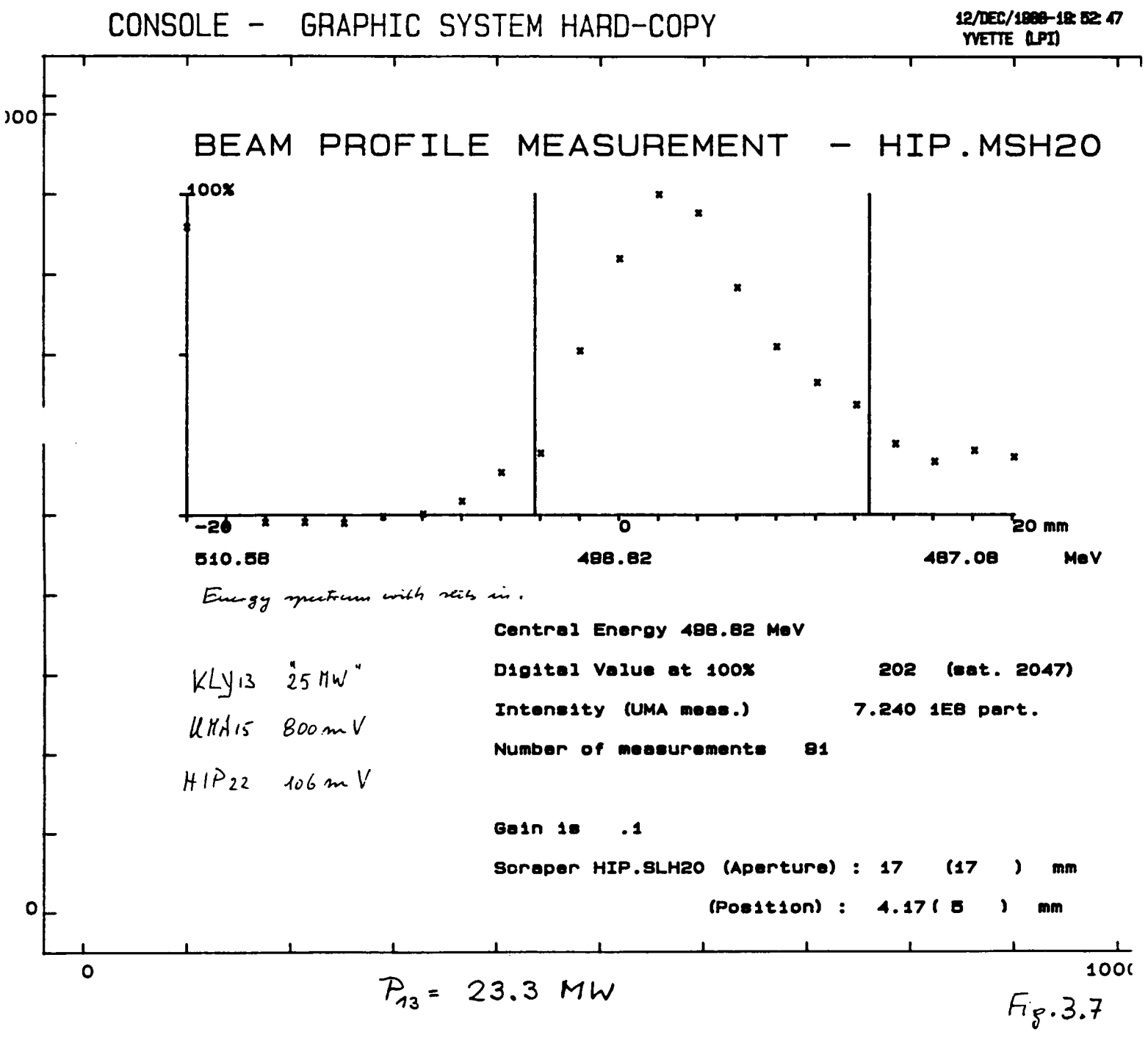
CONSOLE - GRAPHIC SYSTEM HARD-COPY
12/DEC/1988-18:52:47
YVETTE (LPI)
BEAM PROFILE MEASUREMENT - HIP.MSH20
100%
-20
0
20 mm
510.58
488.82
487.08
MeV
Energy spectrum with slits in.
KLY13 "25 MW"
UMA15 800 mV
HIP22 106 mV
Central Energy 488.82 MeV
Digital Value at 100% 202 (sat. 2047)
Intensity (UMA meas.) 7.240 1E8 part.
Number of measurements 81
Gain is .1
Scraper HIP.SLH20 (Aperture) : 17 (17 ) mm
(Position) : 4.17( 5 ) mm
0
0
100
P13 = 23.3 MW

Fig. 3.7

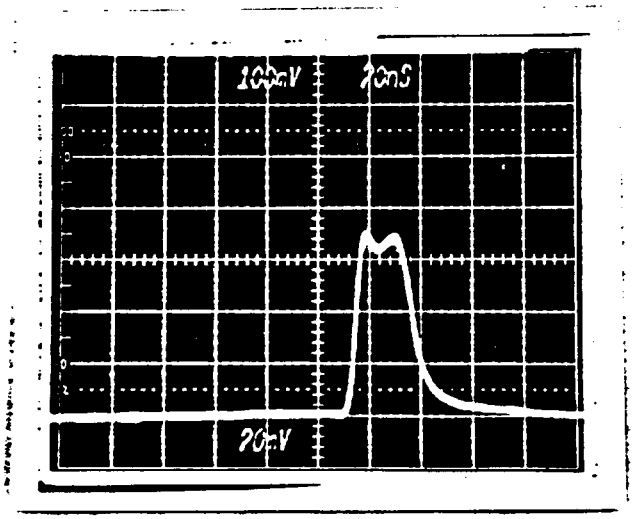


Slits ± 1% in

intensity of primary

beam : $\Sigma_{15} = 0.5\,V$

$\equiv 1.5\,A$

**Fig. 3.8**

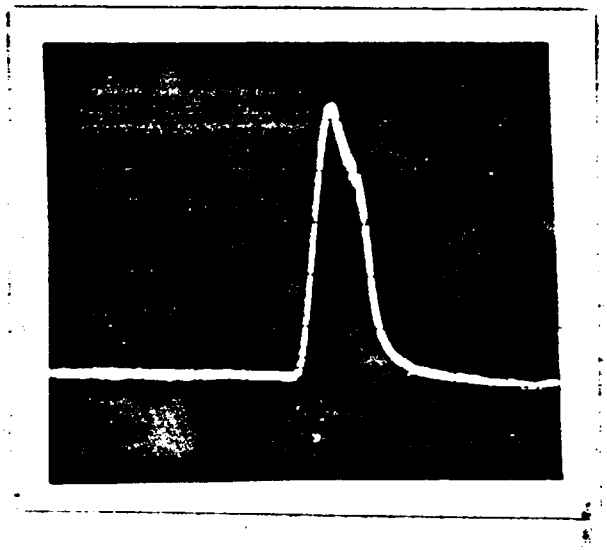

Slits ± 1% in

for $\Sigma_{15} = 0.8\,V$

$\equiv 2.4\,A$

**Fig. 3.9**

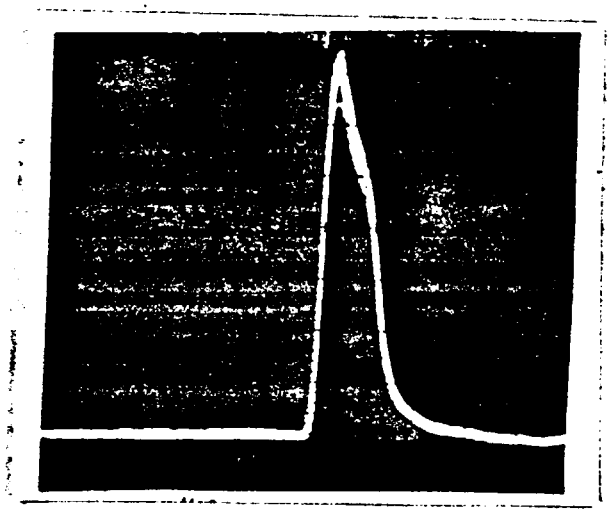

Stits out

for $\Sigma_{15} = 0.8\,V$

$\equiv 2.4\,A$

**Fig. 3.10**

All photos show the analogue signal

of $\Sigma$ (HIP. UMA 22) 20 mV / Div $\equiv$ 1.24 mA / Div

at $P_{13} = 15$ MW 20 ns / Div